Mem. S.A.It. Vol. 87, 237

Memorie della

S-process nucleosynthesis in AGB models with the FST prescription for convection

A. Yagüe[1,2,3], D.A. García-Hernández[2,3], P. Ventura[1], and M. Lugaro[4,5]

[1] Istituto Nazionale di Astrofisica – Osservatorio Astronomico di Roma, Via Frascati 33, 00078 Monte Porzio Catone (RM), Italy, e-mail: andres.lopez@oa-roma.inaf.it
[2] Instituto de Astrofísica de Canarias, C/Vía Láctea s/n, E-38205, Tenerife, Spain
[3] Departamento de Astrofísica, Universidad de La Laguna (ULL), E-38206, Tenerife, Spain
[4] Konkoly Observatory, Hungarian Academy of Sciences, PO Box 67, H-1525 Budapest, Hungary
[5] Monash Centre for Astrophysics, Monash University, VIC3800, Australia

Abstract. The chemical evolution of asymptotic giant branch (AGB) stars depends greatly on the input physics (e.g., mass loss recipe, convective model). Variations in the hot bottom burning (HBB) strength, third dredge-up (TDU) efficiency and AGB evolutionary timescale are among the main consequences of adopting different input physics. The ATON evolutionary code stands apart from others in that it uses the Blöcker mass loss prescription and the Full Spectrum of Turbulence (FST) convective model. We have developed an *s*-process module for ATON by extending the element network from 30 to 320 elements, which uses the physical inputs (such as temperature or density) calculated by ATON. Here we present the first preliminary results of *s*-process nucleosynthesis for ATON AGB models with different progenitor masses. These preliminary results are compared with predictions from other AGB nucleosynthesis models that use different input physics. We also outline our future tasks to improve the current *s*-process ATON simulations.

Key words. Stars: abundances – Stars: AGB and post-AGB – Stars: evolution – Stars: interiors – Nuclear reactions, nucleosynthesis, abundances

1. Introduction

In the world of computer simulations assumptions and simplifications can have a great impact on the results. Asymptotic giant branch (AGB) evolutionary models are not an exception to this. The simulated hot bottom burning (HBB) strength, third dredge-up (TDU) efficiency and AGB evolutionary timescale are some of the physical processes that can be strongly affected by the input physics such as the mass loss prescription and the adopted model for convection (Mazzitelli et al. 1999; Karakas & Lattanzio 2014). These differences in the simulated behaviour of physical mechanisms have, in turn, an effect on the modelled AGB chemical abundance yields, which can be observed. It is therefore of interest to perform numerical experiments in order to understand more about the nature of these stars.

Among the different AGB evolutionary codes used in the literature (e.g., ATON: Ventura et al. 2008; MONASH: Karakas 2010; FRANEC: Straniero et al. 1997; Cristallo et al. 2009; EVOL: Blöcker 1995; Herwig 2000) ATON stands appart in that it uses as standard a combination of the Blöcker mass loss prescription and the Full Spectrum of Turbulence (FST) convective model. However, ATON has so far lacked the capability of performing the nucleosynthesis due to slow neutron captures (the *s*-process), limiting the chemical information to just 30 species. To enable a richer output to study the dependence of the *s*-process nucleosynthesis on different input physics, we built an ATON module for *s*-process nucleosynthesis including 320 nuclear species up to Pb and Bi (Yagüe et al., in preparation). The network is the same as that of Lugaro et al. (2012, 2014) and includes neutron capture rates and β-disintegrations, which are essential for the *s*-process simulations.

2. S-process module design

For this *s*-process module we have opted for a post-processing approach where we use ATON models physical output (temperature and density) and employ the same convective criterion to perform the chemical mixing and burning.

2.1. Chemical mixing

There are two mixing effects in our post-processing code which change the chemical distribution. One is convective mixing, which is performed instantaneously (as opposed to diffusively). The other is overshooting, which is also performed non-diffusively, but keeping an abundance profile (akin to a partial mixing zone). A detailed explanation of the overshooting mechanism implemented in ATON (in which we have based the implementation in our post-processing code) can be found in Ventura et al. (1998).

From these two mixing processes, the overshooting one might be the least consistent with ATON. The different implementations in ATON and in the post-processing (*s*-process) code might give us a slightly inconsistent physics for our chemical profiles in the nucleosynthesis step. However, we do not expect this to be determinant for the evolution of the *s*-process species.

2.2. Chemical burning

The numerical problem arising from *s*-process simulations is characterized by a large (~300) system of first-order non-linear stiff ordinary differential equations (ODEs). This stiffness (exemplified by Fig. 1) forces us to turn our attention to implicit or semi-implicit methods. In Longland et al. (2014) we found a comparison of three of such schemes, out of which we have found that the Bader-Deuflhard method had the best performance for our selection of parameters (Bader & Deuflhard 1983).

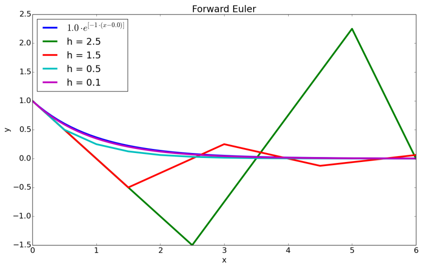

Fig. 1. Example of the stiff ODE y" = -y. The dark blue line represents the analytical solution to the equation. The other lines represent numerical solutions using Forward Euler's method with different step sizes (h). Notice that for h > 2 the numerical solution is unstable.

In order to speed up the algorithm we do not update the jacobian at each substep and we take advantage of its sparsity. We also allow the code to reach a number of substeps before reducing the base timestep higher than in Longland et al. (2014) (from 50 to 4114, which in our tests appeared to be the optimum value for these simulations). This change means that our code performs fewer expensive jacobian inversions per timestep at the cost of performing more backwards substitutions, as well as allowing us to work with larger timesteps.

Finally, we successfully tested our integration code against the results produced by MONASH models which use the same nuclear network.

Table 1. S-process AGB nucleosynthesis results and comparison with van Raai et al. (2012)[a]

Ratio	3 $M_\odot$	4 $M_\odot$	5 $M_\odot$	4 $M_\odot$*	5 $M_\odot$*	6 $M_\odot$*
[Rb/Fe]	0.06	0.03	0.01	0.01 (0.03)	0.05 (0.33)	0.21 (0.73)
[Zr/Fe]	0.06	0.03	0.02	0.01 (0.03)	0.01 (0.16)	0.07 (0.46)
[Rb/Zr]	0.00	0.00	-0.01	0.00 (0.00)	0.03 (0.17)	0.14 (0.27)
[^{87}Rb/^{85}Rb]	0.02	-0.01	0.00	0.01 (0.02)	0.07 (0.37)	0.25 (0.61)

[a]The columns marked with asterisks correspond to the van Raai et al. (2012) data where we are showing the values predicted without the presence of a ^{13}C pocket. The values in parenthesis (in better agreement with observations, see Table 2; Zamora et al. 2014) are those predicted for the same simulation after a synthetic AGB extension.

3. ATON *s*-process preliminary results

We performed eighteen *s*-process simulations for 3, 4 and 5 $M_\odot$ stellar models at solar metallicity with ~10 mesh points in the ^{13}C pocket, which is a thin region in the He-rich intershell where partial mixing leads to the formation of the neutron source nuclei ^{13}C, a mass loss parameter of 0.1 and overshooting parameters of 0.0, 0.2, 0.4, 0.6, 0.8 and 1.2. Curiously, we found our preliminary simulations to show little dependence on the overshooting parameter and the results presented here are those obtained with an overshooting parameter of 1.2 (which we recognize it may be unrealistically high).

Our preliminary results for the Rb and Zr abundances in the three different simulations of 3, 4 and 5 $M_\odot$ AGBs are shown in Table 1, where we compare also with the MONASH models from van Raai et al. (2012). The MONASH models use the Vassiliadis & Wood (1993) recipe for mass loss and the standard mixing length theory (MLT) for convection (see also Karakas 2010 for more details). We have chosen Rb and Zr due to two main reasons: first, they are key species for the *s*-process site (e.g., Abia et al. 2001; García-Hernández et al. 2006) and thus of the progenitor mass of AGB stars (^{22}Ne is expected to be the dominant neutron source in the more massive AGB stars; say > 3-4 $M_\odot$); second, they can be measured from spectroscopic observations of AGB stars with different progenitor masses (e.g., Abia et al. 2001; García-Hernández et al. 2006, 2007). From Table 1 we can see that, although slightly present, the Rb and Zr abundances in our models are lower (by ~0.2 - 0.3 dex in the most massive models) than those from van Raai et al. (2012); our Rb and Zr abundances are near the lower end of the abundance ranges given by these authors, which depend on the size of the ^{13}C pocket and the inclusion of synthetic extended AGB evolution. Also, our Rb and Zr predictions are much lower (up to ~0.5 - 1.0 dex in Rb for the most Rb-rich stars and ~0.1 - 0.3 dex in Zr) than the most actual Rb and Zr abundances measured in solar metallicity massive AGB stars of our Galaxy (Zamora et al. 2014) and shown in Table 2.

4. Discussion

Our preliminary ATON *s*-process nucleosynthesis results show very little *s*-process element enhacements at the stellar surface. A schematic view of the last models for the 3 $M_\odot$ (left panel) and the 5 $M_\odot$ (right panel) simulations are shown in Fig. 2. The lack of *s*-process overabundances may simply be due to inefficient TDU in our models although other effects may also be at play such as e.g., a non appropriate spatial sampling in the intershell region (see below).

To check the efficiency of the TDU in these models, we can calculate the abundances if the intershell values were completely homogenized with the envelope. For example, in the 3 $M_\odot$ case, a "totally" homogenized intershell would give us surface abundances of [Rb/Fe] ~ 0.5 and [Zr/Fe] ~ 0.6 dex, while in the 5 $M_\odot$ case they go down to ~0.1 and ~0.2 dex,

Table 2. Observed abundances of Rb and Zr in massive Galactic AGB stars[a]

IRAS name	05098-6422	06300+6058	18429-1721	19059-2219
[Rb/Fe]	0.0 ± 0.4	0.5 ± 0.7	1.0 ± 0.4	0.8 ± 0.7
[Zr/Fe]	≤ 0.3 ± 0.3	≤ 0.1 ± 0.3	≤ 0.3 ± 0.3	≤ 0.3 ± 0.3
[Rb/Zr]	−0.3 ± 0.7	0.4 ± 1.0	0.7 ± 0.7	0.5 ± 1.0

[a]Rb and Zr abundances from Zamora et al. (2014) where they have used more realistic dynamical atmosphere models for AGB stars than in previous studies (García-Hernández et al. 2006, 2007, 2009).

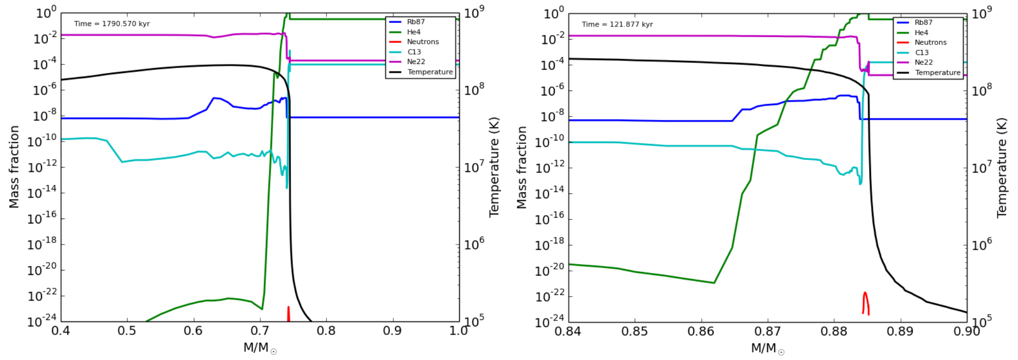

Fig. 2. The last model for our 3 M⊙ (left panel) and 5 M⊙ (right panel) simulations is shown. In these models can be appreciated that, although there has been a moderate Rb enrichment in the intershell, it had almost no impact in the convective envelope abundance. The enriched region size and the envelope size of these models allow us to calculate the approximate abundances in the surface should we mix completely the intershell into the convective envelope (see text).

respectively. This means that although we are producing some abundances of the *s*-process elements in the intershell, they are not being efficiently transported to the stellar surface.

In the comparison with the van Raai et al. (2012) predictions we also have to keep in mind that the minimum progenitor mass for the activation of HBB (∼5 M⊙) in their models is higher than ours; ATON reaches higher temperatures at the bottom of the convective envelope, predicting the activation of HBB for a lower progenitor mass of ∼3.5 M⊙. Thus, our 3, 4 and 5 M⊙ models may find a van Raai et al. (2012) counterpart in their 4, 5 and 6 M⊙ models, respectively.

A solution to reach higher Rb and Zr overabundances at the stellar surface (in better agreement with the observations; see Table 2) might be to use a more efficient TDU (which would imply a change in ATON models) or a stronger overshooting in our simulations (which would imply a bigger ^{13}C pocket). On the other hand, we could also extend the AGB lifetime by changing the mass loss prescription, allowing for more thermal pulses and dredge-up episodes to occur. However, the slight dependence of our *s*-process nucleosynthesis results with the overshooting parameter and with the stellar mass (the activation of the ^{13}C and ^{22}Ne neutron sources) suggests that a numerical problem such as the intershell spatial resolution may be affecting our preliminary simulations. We have used a low-resolution for the intershell region (∼10 mesh points for the ^{13}C pocket) that is likely affecting the chemical evolution of the models. As we can see in Fig. 3 (where a ∼40 mesh points ^{13}C pocket is shown), the ^{13}C pocket and the ^{14}N maximum form in close proximity to each other (see Goriely & Mowlavi 2000; Lugaro et al.

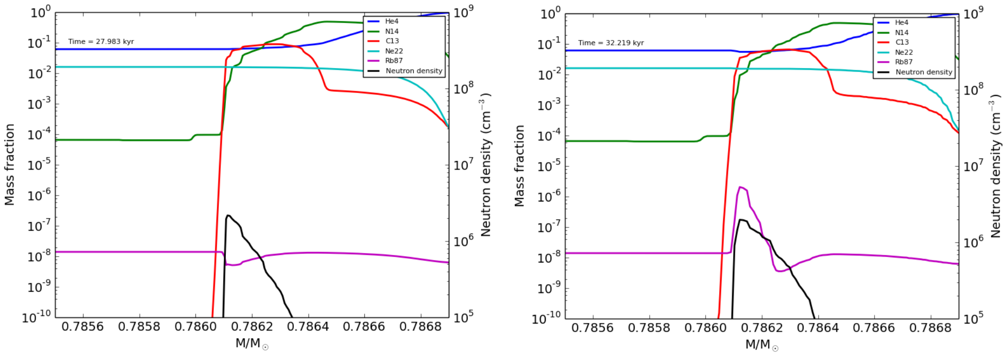

Fig. 3. These two panels represent two different evolutionary points (spanning four thousand years) of the ^{13}C pocket region in a high spatial resolution 4 M$_\odot$ AGB simulation. At the beginning (left panel) the neutron density increases due to the ^{13}C(α, n)^{16}O reaction (Karakas & Lattanzio 2014). This, in turn, affects the *s*-process abundances, here represented by ^{87}Rb (right panel). The proximity of the ^{13}C pocket to the ^{14}N rich zone is the reason why it is important to have enough spatial resolution in this region (see text for more details).

2003; Cristallo et al. 2009). Considering the fact that the ^{14}N is a neutron poison (Karakas & Lattanzio 2014), the neutron density will only grow in the gap between these two maxima (Fig. 3). This means that if the ^{13}C is poorly sampled this gap could disappear completely, inhibiting the neutron density peak, which is fundamental for the *s*-process nucleosynthesis. We conclude that in our models we need a much higher spatial resolution in the intershell region (i.e., near and in the ^{13}C pocket region). Indeed, on-going simulations using higher intershell spatial resolutions predict much higher levels of Rb and Zr at the stellar surface, even for much lower (and more realistic) overshooting parameters (Yagüe et al., in preparation).

5. Summary and future work

We have performed several *s*-process nucleosynthesis preliminary simulations for the ATON evolutionary code in the range of the massive (3-5 M$_\odot$) HBB AGBs at solar metallicity. We have then compared these preliminar predictions with the most recent Rb and Zr abundances determination in massive Galactic AGB stars as well as with other AGB nucleosynthesis models. Our preliminary models give somewhat inconsistent results (e.g., non dependence with the overshooting strength and progenitor mass) and do not match the observations and current models predictions for Rb and Zr. We explored possible causes for this mismatch and we identify the low intershell spatial resolution used as the most likely reason. In the near future, we plan to use much higher spatial resolutions, different mass loss prescriptions and TDU efficiencies. We will also extend these simulations to the whole AGB mass range (1-8 M$_\odot$) and other metallicities.

Acknowledgements. AYL and DAGH acknowledge support provided by the Spanish Ministry of Economy and Competitiveness (MINECO) under the grants AYA-2011-27754 and AYA-2014-58082-P. ML is a Momentum ("Lendület-2014" Programme) project leader of the Hungarian Academy of Sciences.

References

Abia, C., et al. 2001, ApJ, 559, 1117
Bader, G. & Deuflhard, P. 1983, Numerische Mathematik, 41, 373
Blöcker, T. 1995, A&A, 297, 727
Cristallo, S., et al. 2009, ApJ, 696, 797
García-Hernández, D. A., et al. 2006, Science, 314, 1751

García-Hernández, D. A., et al. 2007, A&A, 462, 711
García-Hernández, D. A., et al. 2009, ApJ, 705, L31
Goriely, S. & Mowlavi, N. 2000, A&A, 362, 599
Herwig, F. 2000, A&A, 360, 952
Karakas, A. I. 2010, MNRAS, 403, 1413
Karakas, A. I. & Lattanzio, J. C. 2014, PASA, 31, e030
Longland, R., et al. 2014, A&A, 563, A67
Lugaro, M. et al. 2003, ApJ, 586, 1305
Lugaro, M., et al. 2012, ApJ, 747, 2
Lugaro, M. et al. 2014, Science, 345, 650
Mazzitelli, I. et al. 1999, A&A, 348, 846
Straniero, O., et al. 1997, ApJ, 478, 332
van Raai, M. A., et al. 2012, A&A, 540, A44
Vassiliadis, E. & Wood, P. R. 1993, ApJ, 413, 641
Ventura, P., et al. 1998, A&A, 334, 953
Ventura, P., et al. 2008, Ap&SS, 316, 93
Zamora, O., et al. 2014, A&A, 564, L4